

Thermodynamic and transport properties of $\text{NiCl}_2\text{-4SC(NH}_2)_2$: role of strong mass renormalization

Y. Kohama,¹ A. V. Sologubenko,² N. R. Dilley,³ V. S. Zapf,¹ M. Jaime,¹ J. Mydosh,⁴ A. Paduan-Filho,⁵ K. Al-Hassanieh,⁶ P. Sengupta,⁷ S. Gangadharaiah,^{8,9} A. L. Chernyshev,^{8,9} and C. D. Batista⁶

¹MPA-CMMS, LANL, Los Alamos, New Mexico 87545, USA

²II. Physikalisches Institut, Universität zu Köln, Zùlpicher Str. 77, 50937 Köln, Germany

³Quantum Design Inc., San Diego, CA 92121, USA

⁴Kamerlingh Onnes Laboratory, Leiden University, 2300RA Leiden, The Netherlands

⁵Instituto de Física, Universidade de Sao Paulo, Brazil

⁶Theoretical Division, Los Alamos National Laboratory, Los Alamos, New Mexico 87545, USA

⁷School of Physical and Mathematical Sciences, Nanyang Technological University, 50 Nayng Avenue, Singapore 639798

⁸Department of Physics and Astronomy, University of California, Irvine, CA 92697, USA

⁹Max-Planck-Institut für Physik komplexer Systeme, Nöthnitzer Str. 38, 01187 Dresden, Germany

(Dated: May 28, 2022)

Several quantum paramagnets exhibit magnetic field-induced quantum phase transitions to an antiferromagnetic state that exists for $H_{c1} \leq H \leq H_{c2}$. For some of these compounds, there is a significant asymmetry between the low- and high-field transitions. We present specific heat and thermal conductivity measurements in $\text{NiCl}_2\text{-4SC(NH}_2)_2$, together with calculations which show that the asymmetry is caused by a strong mass renormalization due to quantum fluctuations for $H \leq H_{c1}$ that are absent for $H \geq H_{c2}$. We argue that the enigmatic lack of asymmetry in thermal conductivity is due to a concomitant renormalization of the impurity scattering.

PACS numbers: 75.10.Jm, 75.40-s, 75.40.Cx

The correspondence between a spin system and a gas of bosons has been very fruitful for describing field-induced ordered phases in a large class of quantum paramagnets [1–5]. In this analogy, a magnetic field H plays the role of the chemical potential, which, upon reaching a critical value H_{c1} , induces a $T = 0$ Bose-Einstein condensation (BEC), provided that the number of bosons is conserved, the kinetic energy is dominant, and the spatial dimension $d > 1$. Such a BEC state corresponds to a canted XY magnetic ordering of the spins.

At the BEC quantum critical point (QCP), the low-energy bosonic excitations have a quadratic dispersion $\omega = k^2/2m^*$, where m^* is the effective mass. This mass is renormalized by quantum fluctuations in the paramagnetic phase $H < H_{c1}$. In magnets with $H_{c1} \ll H_{c2}$ the renormalization can be expected to be very strong because of the proximity to the magnetic instability. The transition at H_{c1} should be contrasted with the second BEC-QCP that takes place at the saturation field H_{c2} [6]. Since the field induced magnetization is a conserved quantity, there are no quantum fluctuations and no mass renormalization for the fully polarized phase above H_{c2} , i.e., the bare mass m can be obtained from the single-particle excitation spectrum at $H \geq H_{c2}$. Thus, quantum paramagnets are ideal for studying mass renormalization effects because the effective and the bare bosonic masses can be obtained from two different QCP's that occur in the same material.

Here we present theoretical and experimental evidence for a strong mass renormalization effect, $m/m^* \simeq 3$, in $\text{NiCl}_2\text{-4SC(NH}_2)_2$ [referred to as DTN]. We will show that the large asymmetry between the peaks in the low-temperature specific heat, $C_v(H)$, in the vicinity of H_{c1} and H_{c2} is closely described by analytical and Quantum Monte Carlo (QMC) calculations. The mass renormalization also explains similar asymmetries observed in other properties of DTN, such as magnetization [7], electron spin resonance [8], sound velocity

[9, 10], and magnetostriction [11]. In a remarkable contrast to these properties, peaks in the low-temperature thermal conductivity, κ , near H_{c1} and H_{c2} do not show any substantial asymmetry. We provide an explanation to this dichotomy by demonstrating that the leading boson-impurity scattering amplitude is also renormalized by quantum fluctuations, effectively canceling mass renormalization effect in κ .

DTN is a quantum magnet with tetragonal crystal symmetry that exhibits a field-induced BEC [7, 8, 12–14] to a very good approximation [15]. The dominant single-ion uniaxial anisotropy $D = 8.9$ K splits the Ni $S = 1$ triplet into an $S^z = 0$ ground state and an $S^z = \pm 1$ excited doublet. The antiferromagnetic exchange coupling between Ni ions is $J_c = 2.2$ K along the c -axis and $J_a = 0.18$ K along the a - and b -axes, while the gyromagnetic factor along the c -axis is $g = 2.26$ [8]. A magnetic field applied along the c -axis lowers the energy of the $S^z = 1$ state producing a $T = 0$ BEC transition at $H_{c1} = 2.1$ T. The long-range order occurs in a dome-shaped region of the $T - H$ phase diagram between H_{c1} and $H_{c2} = 12.5$ T and below the maximum ordering temperature $T_{max} \simeq 1.2$ K [12]. The $T^{3/2}$ dependence of the critical field expected for a BEC-QCP has been established via direct measurements of the phase boundary with ac susceptibility down to 1 mK [14], and by magnetization measurements [16]. The asymmetry between H_{c1} and H_{c2} [7–12] can also be seen directly in the skewed shape of the phase diagram [12].

The Hamiltonian describing the $S = 1$ spin degrees of freedom of DTN in external field is given by [8]

$$\mathcal{H} = \sum_{\mathbf{r}, \nu} J_\nu \mathbf{S}_{\mathbf{r}} \cdot \mathbf{S}_{\mathbf{r}+\mathbf{e}_\nu} + D \sum_{\mathbf{r}} (S_{\mathbf{r}}^z)^2 - h \sum_{\mathbf{r}} S_{\mathbf{r}}^z, \quad (1)$$

where \mathbf{e}_ν are the primitive vectors of the lattice, $\nu = \{a, b, c\}$, and $h = g\mu_B H$. We introduce Schwinger bosons associated

with the fundamental representation of SU(3) that obey the constraint $\sum_m b_{\mathbf{r}m}^\dagger b_{\mathbf{r}m} = 1$. The subscript $m = \{\downarrow, 0, \uparrow\}$ labels the eigenstates of $S_{\mathbf{r}}^z$ with the eigenvalues $\{-1, 0, 1\}$. The spin operators in this representation are:

$$S_{\mathbf{r}}^z = n_{\mathbf{r}\uparrow} - n_{\mathbf{r}\downarrow}, \quad S_{\mathbf{r}}^+ = (S_{\mathbf{r}}^-)^\dagger = \sqrt{2} \left(b_{\mathbf{r}\uparrow}^\dagger b_{\mathbf{r}0} + b_{\mathbf{r}0}^\dagger b_{\mathbf{r}\downarrow} \right), \quad (2)$$

with $n_{\mathbf{r}m} = b_{\mathbf{r}m}^\dagger b_{\mathbf{r}m}$. We enforce the constraint by introducing spatially uniform Lagrange multiplier μ

$$\hat{\mathcal{H}} = \mathcal{H} + \mu \sum_{\mathbf{r}} \left(b_{\mathbf{r}\uparrow}^\dagger b_{\mathbf{r}\uparrow} + b_{\mathbf{r}\downarrow}^\dagger b_{\mathbf{r}\downarrow} + b_{\mathbf{r}0}^\dagger b_{\mathbf{r}0} - 1 \right). \quad (3)$$

The lowest energy state in the $H < H_{c1}$ paramagnetic regime is $b_{\mathbf{r}0}^\dagger |0\rangle$ and the ground state corresponds to a non-zero expectation value of the $S^z = 0$ boson: $b_{\mathbf{r}0}^\dagger = b_{\mathbf{r}0} = s$. By using the spin representation (2) with the mean-field value for $b_{\mathbf{r}0}^{(\dagger)}$ and neglecting higher-order terms in powers of $b_{\mathbf{r}0}^{(\dagger)}$, we obtain the Hamiltonian in the harmonic approximation

$$\hat{\mathcal{H}} = E_0 + \sum_{\mathbf{k}, \sigma} \left[A_{\mathbf{k}\sigma} \hat{b}_{\mathbf{k}\sigma}^\dagger \hat{b}_{\mathbf{k}\sigma} + \frac{B_{\mathbf{k}}}{2} \left(\hat{b}_{\mathbf{k}\sigma}^\dagger \hat{b}_{-\mathbf{k}\bar{\sigma}}^\dagger + \text{H.c.} \right) \right], \quad (4)$$

with $A_{\mathbf{k}\sigma} = (\mu + s^2 \epsilon_{\mathbf{k}} - h_\sigma)$ and $B_{\mathbf{k}} = s^2 \epsilon_{\mathbf{k}}$, where $E_0 = N(\mu - D)(s^2 - 1)$ is the bare ground-state energy, N is the number of sites, $\sigma = \{\uparrow, \downarrow\}$, $h_\sigma = \pm h$, $\bar{\sigma} = -\sigma$, $\hat{b}_{\mathbf{k}\sigma}^{(\dagger)}$ are the Fourier transformed bosonic operators, and $\epsilon_{\mathbf{k}} = 2 \sum_{\nu} J_{\nu} \cos k_{\nu}$. The anomalous terms indicate that bosons with opposite S^z are created and annihilated in the ground state. These are the quantum fluctuations that lead to renormalization of the quasi-particle dispersion relation. The Hamiltonian (4) is diagonalized by the Bogolyubov transformation

$$\hat{b}_{\mathbf{k}\sigma} = u_{\mathbf{k}} \beta_{\mathbf{k}\sigma} + v_{\mathbf{k}} \beta_{-\mathbf{k}\bar{\sigma}}^\dagger, \quad (5)$$

where $u_{\mathbf{k}} v_{\mathbf{k}} = B_{\mathbf{k}} / 2 \omega_{\mathbf{k}}^0$, $u_{\mathbf{k}}^2 + v_{\mathbf{k}}^2 = (\mu + s^2 \epsilon_{\mathbf{k}}) / \omega_{\mathbf{k}}^0$, and $\omega_{\mathbf{k}}^0 = \sqrt{\mu^2 + 2\mu s^2 \epsilon_{\mathbf{k}}}$. The resultant diagonal form of $\hat{\mathcal{H}}$ is

$$\hat{\mathcal{H}} = \tilde{E}_0 + \sum_{\mathbf{k}} \left[(\omega_{\mathbf{k}}^0 - h) \beta_{\mathbf{k}\uparrow}^\dagger \beta_{\mathbf{k}\uparrow} + (\omega_{\mathbf{k}}^0 + h) \beta_{\mathbf{k}\downarrow}^\dagger \beta_{\mathbf{k}\downarrow} \right]. \quad (6)$$

Thus, the low-energy spectrum for $h < h_{c1}$ is $\tilde{\omega}_{\mathbf{k}}^< \equiv \omega_{\mathbf{k}}^0 - h$. The band $\tilde{\omega}_{\mathbf{k}}^<$ has a minimum at the antiferromagnetic wave-vector $\mathbf{Q} = (\pi, \pi, \pi)$ with the gap $\Delta^< = \omega_{\mathbf{Q}}^0 - h$, whose vanishing point defines the critical field $h_{c1} = g\mu_B H_{c1} = \omega_{\mathbf{Q}}^0$. The ground state energy is also affected by quantum fluctuations:

$$\tilde{E}_0 = E_0 + \sum_{\mathbf{k}} (\omega_{\mathbf{k}}^0 - \mu - s^2 \epsilon_{\mathbf{k}}). \quad (7)$$

The saddle point conditions, $\partial \tilde{E}_0 / \partial s = \partial \tilde{E}_0 / \partial \mu = 0$, lead to the self-consistent equations for the parameters s and μ ,

$$s^2 = 2 - \frac{1}{N} \sum_{\mathbf{k}} \frac{\mu + s^2 \epsilon_{\mathbf{k}}}{\omega_{\mathbf{k}}^0}, \quad D = \mu + \frac{\mu}{N} \sum_{\mathbf{k}} \frac{\epsilon_{\mathbf{k}}}{\omega_{\mathbf{k}}^0}. \quad (8)$$

Using the Hamiltonian parameters for DTN given in Ref. [8], the resulting values are $s^2 = 0.92$ and $\mu = 10.3\text{K}$.

This low-energy theory is valid only for $H \leq H_{c1}$. For $H \geq H_{c2}$ spins are fully polarized and the spectrum can be computed exactly. Since there are no quantum fluctuations for $H \geq H_{c2}$, the exact value of h_{c2} is $h_{c2} = g\mu_B H_{c2} = D - 2\epsilon_{\mathbf{Q}}$, while the unrenormalized excitation spectrum is $\tilde{\omega}_{\mathbf{k}}^> \equiv \epsilon_{\mathbf{k}} - \epsilon_{\mathbf{Q}} + h - h_{c2}$, which also has a minimum at \mathbf{Q} with the gap $\Delta^> = h - h_{c2}$. Since only the excitations near $\mathbf{k} = \mathbf{Q}$ are important at low temperatures, we define the mass tensors for $H < H_{c1}$ and $H > H_{c2}$ as:

$$\frac{1}{m_{\nu\nu}^*} = \left. \frac{\partial^2 \tilde{\omega}_{\mathbf{k}}^<}{\partial k_{\nu}^2} \right|_{\mathbf{k}=\mathbf{Q}}, \quad \frac{1}{m_{\nu\nu}} = \left. \frac{\partial^2 \tilde{\omega}_{\mathbf{k}}^>}{\partial k_{\nu}^2} \right|_{\mathbf{k}=\mathbf{Q}}. \quad (9)$$

Then the mass renormalization factor is given by

$$\frac{m_{\nu\nu}}{m_{\nu\nu}^*} = s^2 \frac{\mu}{\omega_{\mathbf{Q}}^0} \approx \frac{H_{c2}}{4H_{c1}} \cdot \left(1 + \sqrt{1 + \frac{8H_{c1}^2}{H_{c2}^2}} \right). \quad (10)$$

For the parameters of the Hamiltonian from Ref. [8], we obtain $m_{\nu\nu} / m_{\nu\nu}^* \simeq 3.2$. Such a large difference of masses must readily demonstrate itself in the strong asymmetry of the C_v vs H curves near H_{c1} and H_{c2} as well as in the slopes of the specific heat dependence on T at the critical fields where $C_v \propto (Tm)^{3/2}$. These theoretical expectations are supported by the experimental $C_v(T, H)$ data shown in Figs. 1 and 2.

The C_p was measured in single crystals of DTN grown from aqueous solutions of thiourea and nickel chloride, with magnetic field applied along the crystalline c -axis. The experimental C_p vs H was obtained using an AC technique [17], while sweeping the magnetic field in a ^3He fridge furnished with a 17 T superconducting magnet system at the National High Magnetic Field Laboratory (NHMFL) and the Los Alamos National Laboratory. We also used the standard thermal relaxation method to obtain C_v vs T with a dilution refrigerator in a 16 T Physical Properties Measurement System at Quantum Design, Inc. A strongly asymmetric C_p vs H is shown in Fig. 1 for fixed temperatures $T = 0.75\text{K}$ (green line) and $T = 0.4\text{K}$ (red line), alongside the results of the QMC simulations of the spin Hamiltonian in Eq. (1) in a $8 \times 8 \times 32$ lattice (solid symbols). The agreement between the QMC results and the experimental data is very good. For the lowest temperature, the asymmetry of the peaks is $C_{p2}/C_{p1} \simeq 6$, close to $(m/m^*)^{3/2} \approx 5.7$ expected from the theory above.

Our C_v vs T experimental data close to H_{c1} (top panel) and H_{c2} (bottom panel) are displayed in Fig. 2 (lines with symbols). The results of the QMC simulations of Eq.(1) at H_{c1} and H_{c2} are shown by the solid lines. The dashed lines correspond to the analytical calculation of $C_v(T)$ for a dilute gas of hard-core bosons [Eq. (6)] that have the spectra given by $\tilde{\omega}_{\mathbf{k}}^<$ and $\tilde{\omega}_{\mathbf{k}}^>$ at H_{c1} and H_{c2} . The on-site boson-boson repulsion is taken into account at the mean-field level by summing the ladder diagrams (see Ref. [3]). Since this approach is only valid for low density of bosons, it agrees closely with the QMC results at low T , but deviates from them at higher temperatures. The very good agreement between the theoretical results and the experimental curves at H_{c1} and H_{c2} confirms *quantitatively* the expected mass renormalization for $H \leq H_{c1}$.

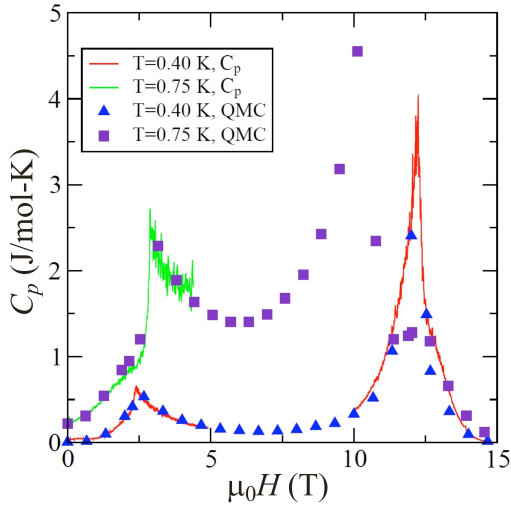


FIG. 1: Specific heat as a function of magnetic field for two temperatures. Measurements and QMC simulations were also performed at the other temperatures showing nearly perfect agreement and the same characteristic behavior of C_p vs H (not included for clarity).

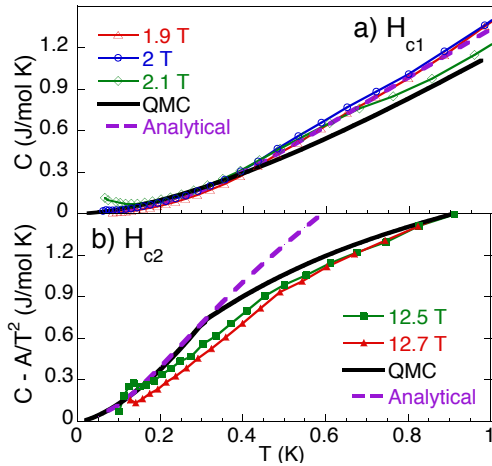


FIG. 2: Specific heat data as a function of T for magnetic fields near (a) H_{c1} and (b) H_{c2} . A Schottky anomaly tail, A/T^2 with $A = 0.018 \text{ J/mol K}^3$, has been subtracted for fields near H_{c2} . The full lines correspond to QMC simulations of Eq.(1) for $H = H_{c1(2)}$ and the parameters of Ref. [8]. The dashed lines are analytical calculations.

The thermal conductivity was measured in DTN single crystals using the standard uniaxial heat flow method, where the temperature difference was produced by a heater attached to one end of the sample and monitored with a matched pair of RuO_2 thermometers. The heat flow and the magnetic field were parallel to the c -axis. Similar observations were reported in Ref. 18 although their data at base temperature (380 mK) do not agree with ours, measured down to 300 mK.

The lighter mass of bosons for $H \leq H_{c1}$ implies not only large asymmetry between the peaks in the specific heat field

dependence, but also similar asymmetries in a number of other properties of DTN [7–11], all exhibiting a much stronger anomaly at H_{c2} than at H_{c1} . In contrast, the low-temperature thermal conductivity *does not* show any substantial asymmetry between the H_{c1} and H_{c2} data. Fig. 3 shows the field dependence of the thermal conductivity, κ , normalized to the $H = 0$ value, $\kappa(0)$, for several low values of T . Since the $H = 0$ magnetic excitation spectrum has a gap of about 3K [8], only phonons contribute to $\kappa(0)$ at low temperatures. The behavior of κ changes qualitatively in the field because the gap is closed between H_{c1} and H_{c2} . The low-temperature magnetic excitations provide a substantial contribution to the thermal conductivity as is clear from $\kappa(H)/\kappa(0) > 1$ in Fig. 3. Here we focus on the low-temperature behavior of κ at the critical points H_{c1} and H_{c2} . A detailed analysis of the other aspects of κ will be provided elsewhere [19].

At low enough temperatures, scattering of bosons on each other should diminish because their concentration will be small. Consequently, the leading scattering in this regime should be due to defects. In the second Born approximation, the disorder-averaged inverse mean-free path of an excitation of mass m due to scattering on point-like impurities is [20]

$$\ell^{-1} = \frac{n_i}{2\pi} |V|^2 m^2, \quad (11)$$

where n_i is the impurity concentration and V is the effective impurity potential. When the excitation gap vanishes at H_{c1} or H_{c2} , thermal conductivity at low- T can be written as

$$\kappa \propto \frac{\ell}{m} \int_0^{\sqrt{mT}} k^3 dk \propto mT^2 \cdot \ell \propto \frac{T^2}{n_i m |V|^2}. \quad (12)$$

The theoretical temperature dependence, $\kappa \propto T^2$, is in a good agreement with the measured low- T thermal conductivity. However, this dependence does not shed any light on the lack of asymmetry between the peaks. Since vacancies or substitutional impurities are expected to be rare in clean enough

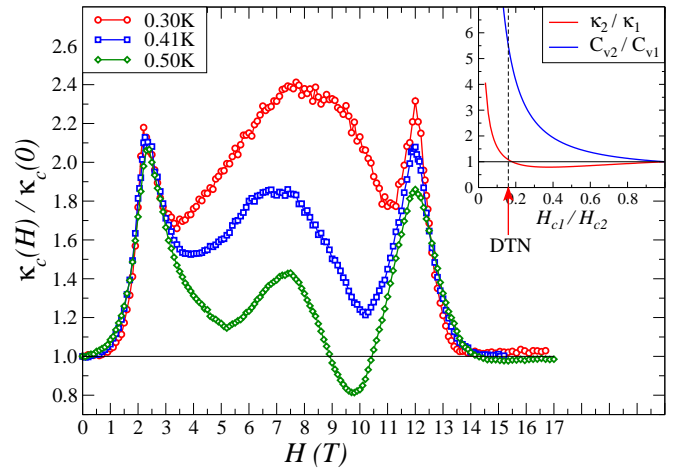


FIG. 3: Thermal conductivity of DTN along the c -axis as a function of magnetic field for several low- T values. Inset: Theoretical prediction for the peak ratios κ_2/κ_1 and C_{v2}/C_{v1} vs H_{c1}/H_{c2} .

systems like DTN, we can assume that random lattice distortions are the most common source of disorder. Because D is the largest parameter in Eq.(1), the most significant effect of these distortions is a real space modulation of D :

$$\mathcal{H}_{\text{imp}}^D = \delta D (S_i^z)^2 \Rightarrow \delta D \sum_{\sigma, \mathbf{k}, \mathbf{k}'} e^{i\mathbf{R}_i(\mathbf{k}-\mathbf{k}')} b_{\mathbf{k}\sigma}^\dagger b_{\mathbf{k}'\sigma}, \quad (13)$$

where \mathbf{i} is the impurity site and we have used the mapping (2).

This is where the renormalization due to quantum fluctuations becomes crucial again. For $H = H_{c2}$ the impurity scattering in (13) is not renormalized due to the absence of quantum fluctuations and $V_2 \equiv \delta D$. On the other hand, for $H = H_{c1}$ the scattering *is* affected by the quantum fluctuations. Since the dressed bosonic excitations are related to the bare ones through Eq. (5), this transforms impurity scattering (13) into

$$\mathcal{H}_{\text{imp}}^D = \delta D \sum_{\sigma, \mathbf{k}, \mathbf{k}'} e^{i\mathbf{R}_i(\mathbf{k}-\mathbf{k}')} (u_{\mathbf{k}} u_{\mathbf{k}'} + v_{\mathbf{k}} v_{\mathbf{k}'}) \beta_{\mathbf{k}\sigma}^\dagger \beta_{\mathbf{k}'\sigma}. \quad (14)$$

Thus, the impurity potential at H_{c1} is $V_1 = \delta D (u_{\mathbf{Q}}^2 + v_{\mathbf{Q}}^2)$, which will modify the mean-free path in (11). After some algebra utilizing Eqs. (12), (5) and (10), we finally obtain

$$\frac{\kappa_2}{\kappa_1} = \frac{m \cdot \ell_2}{m^* \cdot \ell_1} = \left(\frac{m}{m^*} \right) \cdot \frac{1}{4s^4} \cdot \left(1 + s^4 \left(\frac{m^*}{m} \right)^2 \right)^2. \quad (15)$$

This expression contains a large prefactor (m/m^*) coming from the renormalization of the density of states and velocity in (12), and would formally imply a larger peak at H_{c2} , similar to the specific heat and other quantities. However, this effect is partially compensated by the numerical factor $\approx 1/4 + O((m^*/m)^2)$, which comes from the renormalization of the mean-free path. By using the DTN parameters, we obtain $\kappa_2/\kappa_1 \approx 1.1$ in an excellent agreement with the data in Fig. 3. Thus, the mass renormalization effect in thermal conductivity is compensated by a similar renormalization effect in the impurity scattering. To show that this is not a mere coincidence, we provide our prediction for the H_{c1}/H_{c2} dependence of the peak ratios in thermal conductivity κ_2/κ_1 and specific heat C_{v2}/C_{v1} on H_{c1}/H_{c2} (see inset in Fig. 3). Here we used the relation between the mass ratio and H_{c1}/H_{c2} given by Eq. (10). The vertical line corresponds to the DTN value of $H_{c1}/H_{c2} \approx 0.17$. It is remarkable that κ_2/κ_1 and C_{v2}/C_{v1} behave in very different ways. In particular, $\kappa_2/\kappa_1 \approx 1$ while the peaks in C_v are very asymmetric for $0.1 \lesssim H_{c1}/H_{c2} \leq 1$. With this insight, we also suggest an experimental verification of our theory by conducting the heat conductivity measurement in DTN under pressure. A modest decrease of H_{c1} by 1T should lead to an increase in κ_2/κ_1 by a factor of 2.

The leading impurity scattering (13) and, consequently, the resulting expression for the ratio κ_2/κ_1 in (15) will remain valid for the other BEC magnets even though they may not be dominated by the single-ion anisotropy term. For instance, in the dimer-based systems [4], the disorder in the leading intra-dimer coupling translates into the local modulation of

the chemical potential which is equivalent to our Eq. (13). Thus, our Eq. (15) can be verified in other BEC compounds.

In conclusion, by using the example of DTN, we connected the asymmetry in the physical properties of BEC magnets with the mass renormalization of the elementary excitations due to quantum fluctuations of the paramagnetic state. We also resolved the enigmatic absence of this asymmetry in the low- T thermal conductivity by identifying the leading scattering mechanism and by demonstrating that the renormalization of the latter compensates the mass renormalization effect.

This work was supported by the NSF, the State of Florida, the US DOE under grant DE-FG02-04ER46174 (A. L. C.) and by the DFG, SFB 608 (A.S. and J.M.).

-
- [1] I. Affleck, Phys. Rev. B **43**, 3215 (1991).
 - [2] T. Giamarchi and A. M. Tsvelik, Phys. Rev. B **59**, 11398 (1999).
 - [3] T. Nikuni, M. Oshikawa, A. Oosawa, and H. Tanaka, Phys. Rev. Lett. **84**, 5868 (2000).
 - [4] M. Jaime, V. F. Correa, N. Harrison, C. D. Batista, N. Kawashima, Y. Kazuma, G. A. Jorge, R. Stern, I. Heinmaa, S. A. Zvyagin, et al., Phys. Rev. Lett. **93**, 087203 (2004).
 - [5] S. E. Sebastian, V. S. Zapf, N. Harrison, C. D. Batista, P. A. Sharma, M. Jaime, I. R. Fisher, and A. Lacerda, Phys. Rev. Lett. **96**, 189703 (2006).
 - [6] E. G. Batyev and L. S. Braginskii, Sov. Phys. JETP **60**, 781 (1984).
 - [7] A. Paduan-Filho, X. Gratens, and N. F. O. Jr., Phys. Rev. B **69**, 020405(R) (2004).
 - [8] S. Zvyagin, J. Wosnitza, C. D. Batista, M. Tsukamoto, N. Kawashima, J. Krzystek, V. S. Zapf, M. Jaime, N. F. O. Jr., and A. Paduan-Filho, Phys. Rev. Lett. **98**, 047205 (2007).
 - [9] O. Chiatti, S. Zherlitsyn, A. Sytcheva, J. Wosnitza, A. A. Zvyagin, V. S. Zapf, M. Jaime, and A. Paduan-Filho, J. Phys. **150**, 042016 (2009).
 - [10] S. Zherlitsyn, O. Chiatti, A. Sytcheva, J. Wosnitza, A. A. Zvyagin, V. S. Zapf, M. Jaime, and A. Paduan-Filho, J. Phys. **145**, 012069 (2009).
 - [11] V. S. Zapf, V. F. Correa, P. Sengupta, C. D. Batista, M. Tsukamoto, N. Kawashima, P. Egan, C. Pantea, A. Migliori, J. B. Betts, et al., Phys. Rev. B **77**, 020404(R) (2008).
 - [12] V. S. Zapf, D. Zocco, B. R. Hansen, M. Jaime, N. Harrison, C. D. Batista, M. Kenzelmann, C. Niedermayer, A. Lacerda, and A. Paduan-Filho, Phys. Rev. Lett. **96**, 077204 (2006).
 - [13] S. A. Zvyagin, J. Wosnitza, A. K. Kolezhuk, V. S. Zapf, M. Jaime, A. Paduan-Filho, V. N. Glazkov, S. S. Sosin, and A. Smirnov, Phys. Rev. B **77**, 092413 (2008).
 - [14] L. Yin, J. S. Xia, V. S. Zapf, N. S. Sullivan, and A. Paduan-Filho, Phys. Rev. Lett. **101**, 187205 (2008).
 - [15] The number of bosons or uniform magnetization is never strictly conserved in real magnets due to spin-orbit interaction.
 - [16] A. Paduan-Filho, K. A. Al-Hassanieh, P. Sengupta, and M. Jaime, Phys. Rev. Letters **102**, 077204 (2009).
 - [17] Y. Kohama, C. Marcenat, T. Klein, and M. Jaime, Rev. Sci. Instrum. (2010).
 - [18] X. F. Sun, W. Tao, X. M. Wang, and C. Fan, Phys. Rev. Lett. **102**, 167202 (2009).
 - [19] A. L. Chernyshev and C. D. Batista, unpublished.
 - [20] G. D. Mahan, *Many-Particle Physics* (Plenum Press, New York, London, 1990).